Acquisition of an Enhanced Aggressive Phenotype in H1299 Human Lung Cancer Cells Selected by Suboptimal Doses of Cisplatin Following Cell Deattachment and Reattachment

Jeng-Long Hsieh [a,1], Chia-Sing Lu [b,1], Chin-Ling Hwang [b], Gia-Shing Shieh [c], Bing-Hua Su [d], Yu-Chu Su [b], Che-Hsin Lee [e], Meng-Ya Chang [f], Chao-Liang Wu [b,*] and Ai-Li Shiau [d,*]

[a] *Department of Nursing, Chung Hwa University of Medical Technology, Tainan Hsien, Taiwan;* [b] *Department of Biochemistry and Molecular Biology, National Cheng Kung University Medical College, Tainan, Taiwan;* [c] *Department of Urology, Tainan Hospital, Department of Health, Executive Yuan, Taiwan;* [d] *Department of Microbiology and Immunology, National Cheng Kung University Medical College, Tainan, Taiwan;* [e] *Department of Microbiology, School of Medicine, China Medical University, Taichung, Taiwan;* [f] *Graduate Institute of Clinical Medicine, Tzu Chi University, Hualien, Taiwan.*

[1] Both authors contributed equally to this work.

[*] Corresponding authors: Ai-Li Shiau, PhD, Department of Microbiology and Immunology, National Cheng Kung University Medical College, 1 University Road, Tainan 70101, Taiwan; Phone: +886-6-2353535 ext. 5629; Fax: +886-6-2363715; E-mail: alshiau@mail.ncku.edu.tw and Chao-Liang Wu, PhD, Department of Biochemistry and Molecular Biology, National Cheng Kung University Medical College, 1 University Road, Tainan 70101, Taiwan; Phone: +886-6-2353535 ext. 5536; Fax: +886-6-2741694; E-mail: wumolbio@mail.ncku.edu.tw

Abbreviations: ABC, ATP-binding cassette; CSC, cancer stem cell; EMT: epithelial-to-mesenchymal transition; IC50: 50% inhibition of proliferation; NSCLC: non-small cell lung carcinoma; OPN: osteopontin; SP: side population

Abstract

Platinum-based chemotherapy is one major approach for treating non-small cell lung carcinoma (NSCLC). However, the progression-free survival rate depends on whether there is tumor metastasis and drug resistance after treatment. The biological behavior for these two characteristics remains to be clarified. Here, we treated H1299 NSCLC cell line with cisplatin at the IC_{50} dose (1 μg/ml). Most attached cells were surviving cells (H1299-A), whereas only a small portion of detached cells survived and reattached to tissue culture plates (H1299-R1) for further growth. A series of sublines (H1299-R2~H1299-R5) were also generated using the same selection procedure. Cisplatin treatment inhibited the adhesion ability of H1299-R cells compared with their H1299 and H1299-A counterparts. H1299-R cells exhibited increased drug resistance to cisplatin, increased invasiveness, metastatic potential, and increased expression of CD44. Compared with mice subcutaneously injected with H1299 cells, mice subcutaneously injected with H1299-R cells showed an increase in the number of metastatic lung nodules. We conclude that H1299-R cells selected by suboptimal doses of cisplatin following detachment from and reattachment to the tissue culture plate acquire an enhanced malignant phenotype. Therefore, they provide a more faithful lung cancer model associated with biological aggressiveness for studying clinically recurrent cancers after chemotherapy.

Keywords: lung cancer, chemoresistance, cell adhesion, metastasis, CD44

1. Introduction

Lung cancer is the leading cause of cancer death worldwide. This disease is categorized as small cell lung carcinoma (SCLC) or non-small cell lung carcinoma (NSCLC). The latter type, which accounts for 80% of lung tumors, has a poor prognosis because of local or distant metastasis. Treatment is decided based upon the stage and type of tumor identified. For patients with early-stage NSCLC, surgical resection is preferred. Most will require chemotherapy even if their initial surgery is potentially curative [1]. A multimodality approach that includes both radiotherapy and chemotherapy has been used to treat patients with locally advanced cancer or metastatic disease.

Tumor recurrence and metastasis are the major causes of unsuccessful lung cancer treatment. Tumor cells resistant to chemotherapy may recur locally and migrate to distal organs via vessels and lymph nodes through the following steps: angiogenesis, de-adhesion, migration, intravasation, and extravasation [2]. Increasing evidence suggests that tumor progression is critically involved with the acquisition of an epithelial-to-mesenchymal transition (EMT) phenotype, which allows tumor cells to acquire the capacity to infiltrate surrounding tissue and to metastasize to distant sites [3]. EMT was first recognized as a transient process characterized by phenotypic and molecular alterations during embryogenesis. It has been suggested that EMT is crucially involved in the conversion of a primary tumor to an invasive tumor [4]. EMT progression is associated with the acquisition of a mesenchymal phenotype accompanied by the loss of epithelial markers and the activation of mesenchymal markers, which leads to increased cell invasion [5, 6]. These processes coincide with the acquisition of cancer stem cell (CSC) characteristics [7]. CSCs are similar to normal stem cells in their ability to self-renew and to generate large populations of more differentiated descendants within tumors. CSCs have been isolated from various types of solid tumors [8-10]. The recurrence and metastasis of tumors is believed to be

strongly linked with the properties of CSCs [11]. Emerging evidence shows that cells with an EMT phenotype induced by different factors are rich sources for CSCs [12, 13], which suggests that CSCs and EMT phenotypic cells share biological similarities. Furthermore, the induction of EMT in tumor cells can lead to drug resistance, which implies that the capacity for drug resistance and metastasis may coexist within a certain subset of tumor cells [14, 15].

Resistance to chemotherapeutic agents available for treating NSCLC is one of the biggest obstacles to improving long-term outcomes for patients. Chemoresistance occurs not only to clinically established therapeutic agents, but also to novel targeted therapeutics, a trait known as multidrug resistance (MDR). Molecular biology studies [16] report the existence of multiple genetic aberrations in tumor cells, such as cell cycle alteration, apoptosis inhibition, DNA repair adducts, and changes in cellular drug accumulation that confer MDR on tumor cells. The ATP-binding cassette transporters (ABC) are transmembrane proteins that facilitate the transport of specific substrates across the membranes of tumor cells [17]. ABC activation in tumors is responsible for pumping multiple cytotoxic cancer drugs out of the cells, thus preventing them from reaching therapeutic level [18].

Cisplatin is one of the most common anti-cancer agents for the treatment of NSCLC [19]. By interacting with DNA, cisplatin inhibits both RNA transcription and DNA replication, and leads to cell cycle arrest and apoptosis. However, the outcome of cisplatin therapy on NSCLC seems to be unsatisfactory because of the acquired or intrinsic resistance of tumor cells to this drug. Here, we proposed that in the cellularly and molecularly heterogeneous lung cancer cells, a subset of tumor cells can exhibit a more invasive phenotype and be relatively resistant to conventional chemotherapy. In a human NSCLC cell line, H1299, treated with cisplatin, very few tumor cells from the suspended cell debris survived and reattached to the culture plate after drug selection. These cisplatin-resistant, reattached cells, H1299-R, were collected and their drug resistance, cell adhesion, and

malignancy were analyzed. Our results may provide some new insights on tumor metastasis and drug resistance in patients who undergo chemotherapy.

2. Materials and Methods

2.1. Cell Lines and Animals

Human lung cancer cell lines H1299 (ATCC CRL-5803) and its sublines, H1299-R1~H1299-R5, were cultured in the complete medium consisting of Dulbecco's modified Eagle's (DMEM), 10% cosmic calf serum (Hyclone, Logan, UT), 2 mM L-glutamine, and 50 μg/ml of gentamicin at 37°C in 5% CO_2. Male C57BL/6 mice at 6-8 weeks of age were purchased from the Laboratory Animal Center of National Cheng Kung University. The experimental protocol adhered to the rules of the Animal Protection Act of Taiwan and was approved by the Laboratory Animal Care and Use Committee of National Cheng Kung University.

2.2 Immunoblotting, Immunofluorescence, and Immunohistochemistry

Total cell lysates were prepared as previously described [20], and then separately probed with mouse antihuman N-cadherin monoclonal antibody (BD Biosciences, Franklin Lakes, NJ), mouse vimentin monoclonal antibody (RV202; BD Biosciences), mouse antihuman snail monoclonal antibody (L70G2; Cell Signaling, Danvers, MA), rabbit antihuman p-Akt and Akt polyclonal antibodies (Cell signaling), rabbit antihuman β-catenin polyclonal antibody (Cell signaling), mouse monoclonal CD44 antibody (8E2) (Cell Signaling), mouse antihuman occludin monoclonal antibody (OC-3F10; Invitrogen, Carlsbad, CA), rat antihuman ABCG2 monoclonal antibody (BXP-53; Abcam, Cambridge, UK), rabbit antihuman osteopontin polyclonal antibody (Abcam), β-actin (AC-15; Sigma-Aldrich, St. Louis, MO), and GAPDH (Santa Cruz Biotechnology, Santa Cruz, CA). The rat CD44 blocking antibody (IM7; eBioscience, San Diego, CA) was used to abolish the function of CD44. For the immunofluorescence analysis, cells grown on a 96-well plate were fixed in 3.7% formalin, permeabilized with 0.5% Triton X-100, incubated with β-catenin and CD44 antibodies at 4°C

overnight, and subsequently incubated with DyLight488-conjugated goat anti-rabbit antibody (Jackson ImmunoResearch Laboratories, West Grove, PA) and fluorescein-conjugated goat anti-mouse antibody (KPL, Gaithersburg, MD), respectively, at room temperature for 1 h. Nuclei were stained with 50 μg/ml of DAPI. The expression and localization of the proteins were observed under a fluorescent microscope. For immunohistochemistry, lung tissue was collected, fixed in 4% formalin, and then embedded in paraffin. Sections were stained with mouse CD44 monoclonal antibody and sequentially incubated with the appropriate peroxidase-labeled secondary antibody and 3-amino-9-ethylcarbazole as the substrate chromogen. The slides were counterstained with hematoxylin.

2.3. Sirius Red Stain

Cells grown on 24-well plates were fixed in 3.7% formalin and stained with 0.1% Sirius red (Sigma-Aldrich) for 1 h. The Sirius red dye was then dissolved from the cells with 0.1 N NaOH/100% methanol, and then the absorbance at 540 nm that stands for the content of type I collagen within the cells was measured.

2.4. Cell Proliferation and Colony Formation Assays

To analyze cell proliferation, 1,000 cells were seeded in 96-well plates in the complete medium at 37°C on day 0. The number of cells was counted daily from day 1 to day 4 using a cytometer (Celigo™ Cytometer; Cyntellect, San Diego, CA) according to the manufacturer's instructions. The proliferation rate is expressed as a ratio of the number of cells counted on days 2, 3, and 4 by the number counted on day 1. For colony formation assays, cells were thoroughly dissociated with 0.1% trypsin to prepare a single-cell suspension. Each well of 6-well plates was covered with a basal layer of 6 ml of 0.5% agarose containing 50% complete medium. After the medium was solidified, 1 ml of 0.35% agarose containing 2,000

cells and 50% complete medium in triplicate was added to each well. These wells were finally covered with 500 μl of complete medium and the plates were incubated at 37°C. The number of cells in each colony was then counted on day 6 and day 20 using the cytometer.

2.5. Cell Motility Assay

Cell invasion was analyzed using Boyden chamber assays with 8-μm pore polycarbonate filters (Neuro Probe, Gaithersburg, MD) coated with 0.1 μg/ml of gelatin (Sigma-Aldrich). The lower chambers containing 28 μl of the complete medium were covered with the filters. Cells were seeded in the upper chambers containing serum-free medium at a density of 2.5×10^4 per well. After 12 h of incubation at 37°C, the cells were fixed with methanol and stained with Giemsa solution (Invitrogen) for 1 h. Cells on the upper surface of the filter were scraped with cotton buds. Invaded cells on the underside of the filter were then photographed and counted using phase contrast microscopy.

2.6. Drug Sensitivity Assay

Cells (1.5×10^3) seeded in 96-well plates were incubated at 37°C. After 24 h, a medium containing cisplatin in various concentrations (0 to 50 μg/ml) was added to each well. After 72 h of incubation, the surviving cells were assessed using the WST-8 assay (Dojindo Labs, Tokyo, Japan). The absorbance at 450 nm that stands for surviving cells was measured with the reference wavelength at 595 nm. The percentage of survival is expressed as a ratio of O.D. values measured at each drug concentration (0.19 to 50 μg/ml) to that of 0 μg/ml. Drug sensitivity was determined as the drug concentration required for 50% inhibition of proliferation (IC_{50}).

2.7. Flow Cytometry

Cells (2×10^6 per analysis) were stained with fluorescein-conjugated rat anti-mouse CD44 monoclonal antibodies (IM7; BD Pharmingen, San Diego, CA) for 1 h at room temperature. The cells were then washed twice with staining buffer and suspended in DMEM-based buffer for flow cytometric analysis.

2.8. Animal Studies

Groups of 4 or 5 mice were subcutaneously inoculated with H1299 or H1299-R5 cells (1×10^6) on day 0. Palpable tumors were measured every week in two perpendicular axes with a tissue caliper, and the tumor volume was calculated as: (length of tumor) × (width of tumor)^2 × 0.45. The mean tumor volumes were calculated only when all the mice within the same group were alive.

2.9. Statistical Analysis

An unpaired, two-tailed Student's *t*-test was used to determine differences between groups to compare collagen production, cell proliferation, the number of migratory cells, colonies formed in soft agar, and tumor volume. A non-parametric Mann-Whitney *U* test was used to compare the number of tumor nodules between groups. Significance was set at $p < 0.05$.

3. Results

3.1 Decreased Expression of Cell Adhesion Molecules and Type I Collagen in H1299-R1 Cells

We treated H1299 cells with cisplatin at the IC_{50} dose (1 μg/ml) for three days. Surviving cells attached to the tissue culture plate, whereas most detached cells underwent apoptosis after treatment. However, a small portion of the suspended cells, which were designated H1299-R1, survived and reattached to the plate for proliferation when cultured in a drug-free medium. Both the drug-resistant attached (H1299-A) and reattached (H1299-R1) cells were collected.

Treatment with cisplatin may aberrantly activate some genes and change their cell adhesion ability. Compared with the H1299-A and H1299 cells, the expression of epithelial-mesenchymal molecules, such as N-cadherin, vimentin, β-catenin, and occludin was lower in H1299-R1 cells. Notably, the expression of Snail protein, an EMT marker, was higher in H1299-R1, especially after induction by cisplatin (Fig. 1A). β-catenin was significantly involved in cell adhesion. The immunofluorescence data revealed that reduced expression of β-catenin on the membrane of H1299-R1 cells may account for the weak cell adhesion (Fig. 1B). In addition, both H1299 and H1299-A cells exhibited a similar morphology seeded on the plate; however, H1299-R1 cells adhered in more-rounded and transparent shapes and displayed a loose appearance with greater gaps between cells under immunofluorescence microscopy (Fig. 2A).

Collagens are one major component of extracellular matrix and are essential elements for cell attachment. H1299-R1 cells stained with Sirius Red showed a reduced aggregation of collagen. It was confirmed that the expression of type I collagen in H1299-R1 cells was significantly lower than that in H1299 and H1299-A cells ($P = 0.0021$ and $P = 0.0062$, respectively, Fig. 2B). Cell-cell adhesion and cell attachment abilities were similar in H1299

and H1299-A cells, but reduced in H1299-R1 cells. Because H1299 and H1299-A cells developed similar phenotypes, we used H1299 cells for the following analysis.

3.2 Increased Resistance to Cisplatin in H1299-R Cells

To enrich the population of reattached cells, we treated H1299-R1 cells with cisplatin for three days. The detached, surviving cells were collected and reattached to the plates. The same procedure was conducted for four times and generated the subsequent H1299-R2, H1299-R3, H1299-R4, and H1299-R5 sublines (the concentrations of cisplatin used for selection were 1, 2, 2, and 2 μg/ml, respectively). Immunoblot analysis revealed that in contrast to the EMT markers, the expression of which was gradually reduced, the expression of p-Akt proteins increased from H1299-R1 to H1299-R5 cells (Fig. 3A). These results indicated that a more specific subpopulation with drug resistance could be selected through this isolation procedure. The chemosensitivity was further evaluated, and the IC_{50} values for the H1299 and H1299-R1~H1299-R5 cells were 1.39, 2.83, 2.76, 2.96, 2.67, and 2.79, respectively (Fig. 3B). H1299-R1 cells were 2.03 times more resistant to cisplatin than their parental cells. ABCG2, one of the ABCs induced by cisplatin, was overexpressed in the H1299-R sublines (Fig. 3C). The elevated expression of ABCG2 potentiated these cells to efflux the drug out of the cells and account for the acquired drug resistance. Because the five sublines (H1299-R1~H1299-R5) developed a similar level of resistance, we used H1299-R5 for the following analysis. The replication rate of H1299-R5 cells was significantly slower than that of H1299 cells (Fig. 3D, $P < 0.0001$). Cells that have the ability to efflux the dye Hoechst 33342 are referred to as "side population" (SP). H1299-R5 cells displayed a higher percentage of SP (0.021% ± 0.067%) than did H1299 cells (0.09% ± 0.047%, $P < 0.0001$, Fig. 3E). These data suggest that after drug selection, a significantly higher fraction of H1299-R cells may survive and become a reservoir for generating new cancer cells.

3.3 Increased Cell Migration and Clone Formation Abilities in H1299-R5 Cells

The other factor that leads to tumor metastasis is the increased migration in addition to the loosened cell adhesion of cancer cells. The H1299-R5 cells migrated more vigorously than did H1299 cells, and more H1299-R5 cells underwent migration than did H1299 cells (861.25 ± 119.44 vs. 737 ± 88.86, $P = 0.033$, Fig. 4A). Additionally, larger and more colonies were formed in H1299-R5 cells than in H1299 cells (Fig. 4B).

3.4 High Level of CD44 Expression in H1299-R Cells

CD44 is a principal receptor of hyaluronate and is vital in cancer cell adhesion and metastasis. The immunoblotting results revealed that the expression of the CD44 total protein was high in the H1299-R sublines, and that it was most abundantly expressed in H1299-R5 cells (Fig. 5A). H1299-R5 cells expressed more CD44 on the cell surface than did H1299 cells (Fig. 5B). Immunofluorescence confirmed that the expression of CD44 on the membrane of H1299-R5 cells was higher and more abundantly than on the membrane of H1299 cells (Fig. 5C). Because osteopontin (OPN) can induce chemoresistance via the CD44 signaling pathway, we analyzed the expression of OPN in H1299-R5 cells. The expression of OPN and ABCG2 was higher in H1299-R5 cells than in H1299 cells (Fig. 5D); however, the expression of both was inhibited when anti-CD44 blocking antibody was present. The increased cell migration and survival abilities of H1299-R5 cells may result in a more aggressive tumor invasion.

3.5 More Invasive Phenotype of H1299-R Cells in Mice

To test the spontaneous metastatic potential of H1299-R5 cells, we subcutaneously injected them (1×10^6) into mice. Tumor development was monitored weekly. The tumors

generated in H1299-group mice were larger (4696.86 ± 3012.38 mm^3) than those in H1299-R5-group mice (591.3 ± 1082.15 mm^3, $P = 0.0049$) on week 9 (Fig. 6A). Although the H1299-R5 cells formed smaller tumors *in situ*, they developed larger tumors in the lungs, indicating a higher level of invasiveness in these cells (Fig. 6B, left). More metastatic tumor nodules were observed in the lung tissue of the H1299-R5-inoculated mice (Fig. 6B, middle). The number of tumor nodules in mice inoculated with H1299-R5 cells was significantly greater than that in mice inoculated with H1299 cells (Fig. 6B, $P = 0.0297$). Furthermore, more intense staining of CD44 was seen in mice inoculated with H1299-R5 cells, suggesting the significance of CD44 in tumor invasion. More tumor nodules were found in mice intravenously inoculated with H1299-R5 cells than with H1299 cells (data not shown). These results suggested that the cisplatin-resistant H1299-R5 cells were more invasive, which might have been attributed to the overexpression of CD44.

4. Discussion

Establishment of drug-resistant lung cancer cell lines with invasive phenotypes is instrumental for developing therapeutic strategies for cancer patients. In the present study, we isolated and enriched a subpopulation of the H1299 cell line, the H1299-R5 cell line, from cell culture. H1299-R5 cells detached from the substratum during cisplatin selection and reattached when the drug was withdrawn. The expression of genes involved in cell adhesion decreased, but the expression of those involved in cell motility and drug efflux increased in H1299-R5 cells. Moreover, these cells have a higher metastatic potential in NOD/SCID mice than H1299 cells. In previous studies [21, 22], the methods used to establish the drug-resistant tumor cell lines were either the transient (24-72 h) or chronic exposure of cells to drugs, and only the adherent surviving cells were collected. The cisplatin-resistant cell lines established in these approaches would keep the same or even lose their ability to metastasize compared with their parental cell lines. This phenomenon suggested that “reverse transformation” can occur in cells. One substantial fraction of surviving cells suspended in the culture medium would be ignored, and their potential involvement in tumor progression would be underestimated. Therefore, we collected the surviving cells from the suspension after the drug had been added. Compared with H1299-A cells, which were selected using the conventional method, H1299-R1 cells showed lower expression levels of genes involved in cell adhesion and collagen type I secretion. The incidence of bone metastasis in lung cancer patients is approximately 30-40% [23]. Metastasis involves a series of de-adhesion and adhesion events, coupled with regulated tissue degradation to facilitate tumor cell migration and spread. Our methods provide a more clinically relevant way to characterize cells that have metastatic potential after chemotherapy. To identify the phenotypes displayed in these cells should provide more insight into the process of metastasis and even the therapeutic targets of lung cancer.

H1299-R1 cells expressed fewer epithelial (β-catenin and occludin) and mesenchymal (N-cadherin and vimentin) markers than did H1229 and H1299-A cells. However, the expression of Snail was higher in H1299-R1 cells particularly in the presence of cisplatin. Whether H1299-R cells underwent EMT remained unclear. Nevertheless, it is recognized that EMT seems not to be a homogenous “black and white” cellular scenario. Snail protein is a transcriptional repressor that belongs to the Snail family, which is critical for cancer cells to acquire radioresistance and chemoresistance. The process is orchestrated through the acquisition of a novel subset of gene targets that effectively inactivates p53-mediated apoptosis, while another subset of targets continues to mediate EMT [24]. Although the H1299 cell line does not have normal p53, Snail may mediate cisplatin resistance through a p53-independent pathway [25, 26].

During serial selection, in contrast to the expression of EMT markers (β-catenin, occludin, and N-cadherin), the expression of p-Akt and Akt increased gradually in the subsequent sublines. This indicated that the reattached cells with the same properties were enriched by repeating the selection procedure. The activation of the antiapoptotic cascade phosphatidylinositol 3-kinase (PI3K)/Akt is important for cell survival. Disseminated tumor cells detected in bone marrow from patients with lung cancer contain activated Akt [27]. Akt activation regulates the proliferation, survival, migration, and EGF-mediated signaling in lung-cancer-derived disseminated tumor cells [27]. Because we used a consistent concentration (2 μg/ml) of cisplatin during the selection, the chemoresistance and the expression of ABCG2 remained unchanged in these sublines. The acquired chemoresistance of H1299-R cells appeared to be involved in increasing cell survival and migration.

CD44 is a membrane-bound glycoprotein, acting as a cell-cell or cell-extracellular matrix adhesion protein. The interaction of CD44 with other cellular proteins, such as hyaluronan, mediates a complex range of functions and has been implicated in tumor

invasion and metastasis [28, 29]. Flow cytometry used to select the CD44-positive cells from several lung cancer cell lines showed that *in vitro* and *in vivo* tumorigenicity were both higher in sorted CD44-positive tumor cells [30]. CD44 consists of various isoforms resulting from alternative splicing of its mRNA. It has been suggested that variant forms of CD44 may participate in cell growth, differentiation, survival, and metastasis, particularly CD44*v*6 [31, 32]. In the H1299-R5 cells, the standard (CD44*s*) and variant forms (CD44*v3,* CD44*v8,* CD44*v9,* and CD44*v10*) all increased compared with H1299 cells (Supplementary Fig. 1). The roles of these isoforms involved in tumor progression require further investigation. Interaction between CD44 and hyaluronate can induce chemoresistance in NSCLC cells [33]. In our study, in addition to CD44, the expression of OPN increased in H1299-R5 cells. OPN is involved in multidrug resistance by increasing CD44 binding to hyaluronate [34]. Furthermore, OPN produced by osteoblasts also bound to CD44 and activated the PIK3/Akt, NF-κB, and matrix metalloproteinase-2 signaling pathway for tumor formation and metastasis [35]. The circulating level of OPN is highly associated with the stage of NSCLC [36]. Consistent with previous data [30, 36], our results suggest that the aberrant expression of CD44 and its ligands within cells when acquiring chemoresistance may be significant for tumor migration and metastasis.

Several recent lines of evidence have suggested that tumor progression is driven by a small population of CSCs, which have the ability to self-renew and to regenerate the phenotypic heterogeneous lineages of cancer cells, thereby initiating tumors and metastasis [37, 38]. Lung cancer progenitor cells, bronchioalevolar stem cells (BASCs), have been identified in healthy lung tissue and lung cancer tissue using a murine model [39]. These cells may be the putative cells of origin for adenocarcinoma. Our results showed that, compared with H1299 cells, the expression of stem-cell markers, OPN, CD44, ABCG2, and SP were all higher in the H1299-R sublines, indicating that there are a higher proportion of CSCs in

H1299-R cells. Indeed, the CD44-expressing subpopulations from some NSCLC cell lines had enriched stem cell-like properties [36]. When anticancer drugs are added, the extracellular stimuli can induce an expansion of a pre-existing stem cell population within tumors through the Snail signaling pathway. Notably, our *in vitro* and *in vivo* results show that the insensitivity of H1299-R cells to cisplatin may cause cancer cells to proliferate at a reduced rate.

The approach we collected cancer cells is different from previously reported methods: first, instead of isolating a single cell, we collected a mixed population of cells with weak cell adhesion; second, instead of maintaining the cells as tumor spheres in a culture system, we re-plated the cells to the substratum to allow further differentiation [40, 41]. When undergoing chemotherapy, some tumor cells with low adhesion ability, including CSCs, detach from the basal lamina, migrate into the circulation, and disseminate to distant sites to reattach. Both of these steps are essential for metastasis. It was reported that the number of circulating tumor cells could be a predictor of overall survival after chemotherapy in patients with various types of cancer [42]. To avoid serious side effects, patients with NSCLC usually received a safer dose of drugs by increasing treatment cycles. This is the reason we used low dose of cisplatin (1 or 2 μg/ml) during H1299-R cells selection. Our method may provide a model more relevant to what actually occurs in cancer patients.

In summary, we have isolated and enriched new cisplatin-resistant lung cancer cell lines that are more aggressive and invasive. These cells may be useful as targets when developing therapeutics for metastatic lung cancer.

Acknowledgements

This work was supported by the National Science Council (NSC 96-3112-B-006-011, NSC 97-3112-B-006-001, and NSC 98-2320-B-006-030-MY3) and the Department of Health, Executive Yuan (DOH 98-TD-G-111-032 and DOH 99-TD-G-111-032), Taiwan.

Conflict of interest

The authors do not have any conflict of interest to disclose.

References

[1] L.G. Collins, C. Haines, R. Perkel, R.E. Enck, Lung cancer: diagnosis and management. Am. Fam. Physician 75 (2007) 56-63.

[2] S.A. Brooks, H.J. Lomax-Browne, T.M. Carter, C.E. Kinch, D.M. Hall, Molecular interactions in cancer cell metastasis. Acta. Histochem. 112 (2010) 3-25.

[3] J.M. Lee, S. Dedhar, R. Kalluri, E.W. Thompson, The epithelial-mesenchymal transition: New insights in signaling, development, and disease. J. Cell Biol. 172 (2006) 973–981.

[4] J.P. Thiery, Epithelial-mesenchymal transitions in tumour progression. Nat. Rev. Cancer 2 (2002) 442–454.

[5] J. Yang, S.A. Mani, J.L. Donaher, S. Ramaswamy, R.A. Itzykson, C, Come, P, Savagner, I, Gitelman, A, Richardson, R,A, Weinberg, Twist, a master regulator of morphogenesis, plays an essential role in tumor metastasis. Cell 117 (2004) 927-39.

[6] B.G. Hollier, K. Evans, S.A. Mani, The epithelial-to-mesenchymal transition and cancer stem cells: A coalition against cancer therapies. J. Mammary Gland Biol. Neoplasia 14 (2009) 29–43.

[7] T. Brabletz, A. Jung, S. Spaderna, F. Hlubek, T. Kirchner, Opinion: migrating cancer stem cells—an integrated concept of malignant tumour progression. Nat. Rev. Cancer 5 (2005) 744–749.

[8] M. Al-Hajj, M.S. Wicha, A. Benito-Hernandez, S.J. Morrison, M.F. Clarke, Prospective identification of tumorigenic breast cancer cells. Proc Natl. Acad. Sci. USA; 100 (2003) 3983-8.

[9] S.K. Singh, C. Hawkins, I.D. Clarke, J.A. Squire, J. Bayani, T. Hide, R.M. Henkelman, M.D. Cusimano, P.B. Dirks, Identification of human brain tumour initiating cells. Nature 432 (2004) 396-401.

[10] S.C. Yu, Y.F. Ping, L. Yi, Z.H. Zhou, J.H. Chen, X.H. Yao, L. Gao, J.M. Wang, X.W. Bian, Isolation and characterization of cancer stem cells from a human glioblastoma cell line U87. Cancer Lett. 265 (2008) 124-34.

[11] S. Kasper, Identification, characterization, and biological relevance of prostate cancer stem cells from clinical specimens. Urol. Oncol. 27 (2009) 301–303.

[12] S.A. Mani, W. Guo, M.J. Liao, E.N. Eaton, A. Ayyanan, A.Y. Zhou, M. Brooks, F. Reinhard, C.C. Zhang, M. Shipitsin, L.L. Campbell, K. Polyak, C. Brisken, J. Yang, R.A. Weinberg, The epithelial-mesenchymal transition generates cells with properties of stem cells. Cell 133 (2008) 704–715.

[13] C.D. May, N. Sphyris, K.W. Evans, S.J. Werden, W. Guo, S.A. Mani, Epithelial-mesenchymal transition and cancer stem cells: a dangerously dynamic duo in breast cancer progression. Breast Cancer Res. 13 (2011) 202.

[14] A. Singh, J. Settleman, EMT, cancer stem cells and drug resistance: an emerging axis of evil in the war on cancer. Oncogene 29 (2010) 4741-51.

[15] Z. Wang, Y. Li, A. Ahmad, A.S. Azmi, D. Kong, S. Banerjee, F.H. Sarkar, Targeting miRNAs involved in cancer stem cell and EMT regulation: an emerging concept in overcoming drug resistance. Drug Resist. Updat. 13 (2010) 109-18.

[16] S.V. Ambudkar, S. Dey, C.A. Hrycyna, M. Ramachandra, I. Pastan, M.M. Gottesman, Biochemical, cellular, and pharmacological aspects of the multidrug transporter. Annu. Rev. Pharmacol. Toxicol. 39 (1999) 361-98.

[17] M.M. Gottesman, T. Fojo, S.E. Bates, Multidrug resistance in cancer: role of ATP-dependent transporters. Nat. Rev. Cancer 2 (2002) 48-58.

[18] M.M. Gottesman, J. Ludwig, D. Xia, G. Szakacs, Defeating drug resistance in cancer. Discov. Med. 6 (2006) 18-23.

[19] H.R. Mirshahidi, C.T. Hsueh, Updates in non-small cell lung cancer-insights from the

2009 45th annual meeting of the American Society of Clinical Oncology. J. Hematol. Oncol. 3 (2010) 18.

[20] J.L. Hsieh, C.L. Wu, C.H. Lee, A.L. Shiau, Hepatitis B virus X protein sensitizes hepatocellular carcinoma cells to cytolysis induced by E1B-deleted adenovirus through the disruption of p53 function. Clin. Cancer Res. 9 (2003) 338-45.

[21] M. Mitsumoto, T. Kamura, H. Kobayashi, T. Sonoda, T. Kaku, H. Nakano, Emergence of higher levels of invasive and metastatic properties in the drug resistant cancer cell lines after the repeated administration of cisplatin in tumor-bearing mice. J. Cancer Res. Clin. Oncol. 124 (1998) 607-14.

[22] G. Bertolini, L. Roz, P. Perego, M. Tortoreto, E. Fontanella, L. Gatti, G. Pratesi, A. Fabbri, F. Andriani, S. Tinelli, E. Roz, R. Caserini, S. Lo Vullo, T. Camerini, L. Mariani, D. Delia, E. Calabrò, U. Pastorino, G. Sozzi, Highly tumorigenic lung cancer CD133+ cells display stem-like features and are spared by cisplatin treatment. Proc. Natl. Acad. Sci. USA. 106 (2009) 16281-6.

[23] A. Tsuya, M. Fukuoka, Bone metastases in lung cancer. Clin. Calcium 18 (2008) 455-9.

[24] N.K. Kurrey, S.P. Jalgaonkar, A.V. Joglekar, A.D. Ghanate, P.D. Chaskar, R.Y. Doiphode, S.A. Bapat, Snail and slug mediate radioresistance and chemoresistance by antagonizing p53-mediated apoptosis and acquiring a stem-like phenotype in ovarian cancer cells. Stem cells 27 (2009) 2059-68.

[25] M. Jiang, C.Y. Wang, S. Huang, T. Yang, Z. Dong, Cisplatin-induced apoptosis in p53-deficient renal cells via the intrinsic mitochondrial pathway. Clin. Exp. Metastasis 296 (2009) F983-93.

[26] T.G. Oliver, K.L. Mercer, L.C. Sayles, J.R. Burke, D. Mendus, K.S. Lovejoy, M.H. Cheng, A. Subramanian, D. Mu, S. Powers, D. Crowley, R.T. Bronson, C.A. Whittaker, A. Bhutkar, S.J. Lippard, T. Golub, J. Thomale, T. Jacks, E.A. Sweet-Cordero, Chronic

cisplatin treatment promotes enhanced damage repair and tumor progression in a mouse model of lung cancer. Genes Dev. 24 (2010) 837-52.

[27] N. Grabinski, K. Bartkowiak, K. Grupp, B. Brandt, K. Pantel, M. Jücker, Distinct, functional roles of Akt isoforms for proliferation, survival, migration and EGF-mediated signalling in lung cancer derived disseminated tumor cells. Cell Signal. 23 (2011) 1952-60.

[28] S. Jothy, CD44 and its partners in metastasis. Clin. Exp. Metastasis 20 (2003) 195-201.

[29] K. Takahashi, I. Stamenkovic, M. Cutler, H. Saya, K.K. Tanabe, CD44 hyaluronate binding influences growth kinetics and tumorigenicity of human colon carcinomas. Oncogene 11 (1995) 2223-32.

[30] E.L. Leung, R.R. Fiscus, J.W. Tung, V.P. Tin, L.C. Cheng, A.D. Sihoe, L.M. Fink, Y. Ma, M.P. Wong, Non-small cell lung cancer cells expressing CD44 are enriched for stem cell-like properties. PLoS One 5 (2010) e14062.

[31] H. Ponta, L. Sherman, P.A. Herrlich, CD44: from adhesion molecules to signalling regulators. Nat. Rev. Mol. Cell Biol. 4 (2003) 33-45.

[32] V.J. Wielenga, R. van der Voort, J.W. Mulder, P.M. Kruyt, W..F Weidema, J. Oosting, C.A. Seldenrijk, C. van Krimpen, G.J. Offerhaus, S.T. Pals, CD44 splice variants as prognostic markers in colorectal cancer. Scand. J. Gastroenterol. 33 (1998) 82-7.

[33] R. Ohashi, F. Takahashi, R. Cui, M. Yoshioka, T. Gu, S. Sasaki, S Tominaga, K. Nishio, K.K. Tanabe, K. Takahashi, Interaction between CD44 and hyaluronate induces chemoresistance in non-small cell lung cancer cell. Cancer Lett. 252 (2007) 225-34.

[34] K. Tajima , R. Ohashi , Y. Sekido , T. Hida , T. Nara , M. Hashimoto , S. Iwakami , K. Minakata , T. Yae , .F Takahashi , H. Saya , K. Takahashi , Osteopontin-mediated enhanced hyaluronan binding induces multidrug resistance in mesothelioma cells. Oncogene 29 (2010) 1941-51.

[35] H. Rangaswami, A. Bulbule, G.C. Kundu, Osteopontin: role in cell signaling and cancer progression. Trends Cell Biol. 16 (2006) 79-87.

[36] Y.S. Chang, H.J. Kim, J. Chang, C.M. Ahn, S.K. Kim, S.K. Kim, Elevated circulating level of osteopontin is associated with advanced disease state of non-small cell lung cancer. Lung Cancer 57 (2007) 373-80.

[37] M.F. Clarke, J.E. Dick, P.B. Dirks, C.J. Eaves, C.H. Jamieson, D.L. Jones, J. Visvader, I.L. Weissman, G.M. Wahl, Cancer stem cells--perspectives on current status and future directions: AACR Workshop on cancer stem cells. Cancer Res. 66 (2006) 9339-44.

[38] C. Sheridan, H. Kishimoto, R.K. Fuchs, S. Mehrotra, P. Bhat-Nakshatri, C.H. Turner, R. Jr. Goulet, S. Badve, H. Nakshatri, CD44+/CD24-breast cancer cells exhibit enhanced invasive properties: an early step necessary for metastasis. Breast Cancer Res. 8 (2006) R59.

[39] C.F. Kim, E.L. Jackson, A.E. Woolfenden, S. Lawrence, I. Babar, S. Vogel, D. Crowley, R.T. Bronson, T. Jacks, Identification of bronchioalveolar stem cells in normal lung and lung cancer. Cell 121 (2005) 823-35.

[40] M.P. Buzzeo, E.W. Scott, C.R. Cogle, The hunt for cancer-initiating cells: a history stemming from leukemia. Leukemia 21 (2007) 1619-27.

[41] L. Yang, Y.F. Ping, X. Yu, F. Qian, Z.J. Guo, C. Qian, Y.H. Cui, X.W. Bian, Gastric cancer stem-like cells possess higher capability of invasion and metastasis in association with a mesenchymal transition phenotype. Cancer Lett. 310 (2011) 46-52.

[42] M.G. Krebs, R. Sloane, L. Priest, L. Lancashire, J.M. Hou, A. Greystoke, T.H. Ward, R. Ferraldeschi, A. Hughes, G. Clack, M. Ranson, C. Dive, F.H. Blackhall, Evaluation and prognostic significance of circulating tumor cells in patients with non-small-cell lung cancer. J. Clin. Oncol. 29 (2011) 1556-63.

Figure Legends

Fig. 1. The expression of EMT markers in cisplatin-resistant H1299-R1 cells. (A) The expression of N-cadherin, vimentin, Snail, β-catenin, and occludin in H1299-R1 and H1299 cells was detected by immunoblotting. β-actin served as the loading control. (B) The distribution of β-catenin was detected on the surface of cells using immunofluorescence (×200 magnification, scale bar = 100 μm, upper; the inset represents the magnified area, ×400 magnification, lower).

Fig. 2. Cisplatin-resistant H1299-R1 cells showed less cell adhesion. (A) The morphology and arrangement of cells was observed after the cells had been stained with Calcium AM (×320 magnification, scale bar = 20 μm). (B) The cells were stained with Sirius Red (×200 magnification, scale bar = 100 μm) and the levels of type I collagen were quantified. Each value represents means of four determinations ± standard deviation (SD), $^{**}P < 0.01$.

Fig. 3. The expression of EMT molecules and chemoresistance against cisplatin in H1299 and five H1299-R sublines. (A) The N-cadherin, β-catenin, occludin, p-Akt, and Akt proteins in H1299-R sublines (H1299-R1~H1299-R5) were detected by immunoblotting. β-actin served as the loading control. (B) The cells were treated with an increasing concentration of cisplatin (from 0 μg/ml to 50 μg/ml) for three days, and cell viability was determined using the WST-8 assay. Each point represents the mean of four determinations ± SD. The IC_{50} value was determined based on the cell survival curve. (C) The expression of ABCG2 was higher in the five H1299-R sublines than in the H1299 cell line. (D) The proliferation rate was slower in H1299-R5 cells than in H1299 cells ($P < 0.0001$). Each point represents the mean of five determinations ± SD. (E) The cells were stained with dye (Hoechst 33342 and Calcium AM) for 30 min. The side population (SP) was the fraction of cells capable of exporting the

Hoechst 33342 out of cells. The percentage of SP is expressed as the ratio of the number of cells free of Hoechst 33342 divided by the total number of cells stained with Calcium AM. Each bar represents the means of twelve determinations ± SD, ***P <0.0001.

Fig. 4. Cell motility and colony formation in H1299-R5 cells. (A) The cell migration was detected using a Boyden chamber assay (Giemsa stain, ×200 magnification, scale bar = 200 μm). The number of migratory cells was quantified, and the data are presented as the means of eight determinations ± SD, *P <0.05. (B) The colonies (arrow heads) were formed on soft agar and the representative results from three randomly chosen areas are shown for day 6 (×40 magnification, scale bar = 500 μm) and day 20 (×40 magnification, scale bar = 200 μm). The number of colonies with different sizes on day 20 (diameter of colony: >400 μm, <400 μm, and <100 μm) in each cell line was quantified.

Fig. 5. Expression of CD44 and OPN in H1299-R5 cells. (A) The CD44 expression in H1299-R sublines was detected by immunoblotting. β-actin served as the loading control. (B) The intensity of CD44 expression on the cell surface was analyzed using flow cytometry. The CD44 expression on the surface of H1299-R5 cells (blue line) and H1299 cells (black line); and the green and red lines represent background fluorescence on H1299-R5 and H1299 cells, respectively. (C) The distribution of CD44 expression on cell membranes was analyzed using immunofluorescence (×200 magnification, scale bar = 50 μm, left; the insets represent the magnified area, ×400 magnification, right). (D) Cells were incubated with 10 μg/ml of anti-CD44 antibody for 4 h. The cultures were then washed five times with PBS, and the proteins were isolated for detecting the expression of OPN and ABCG2 proteins by immunoblotting. GAPDH served as the loading control.

Fig. 6. Increased invasion and CD44 expression of H1299-R5 cells in mice. (A) Cells were subcutaneously injected into NOD/SCID mice on week 0, and the differences in the tumor volumes (means ± SD, n = 5 in the H1299 group and n = 4 in the H1299-R5 group) between the two groups were compared on week 9. (B) The lung tissue was removed on week 9, and representative samples of the macroscopic and histologic appearance of lung tissue were shown (hematoxylin and eosin stain). The number of metastatic nodules was counted and assessed using the Mann-Whitney *U*-test, $*P < 0.05$. (C) The expression of CD44 was detected using anti-CD44 antibody (hematoxylin and eosin stain, ×100 magnification, scale bar = 20 μm, left; immunohistochemical staining, ×100 magnification, scale bar = 20 μm, middle; the insets represent the magnified area, ×200 magnification, scale bar = 20 μm, right).

Figure 1

Click here to download high resolution image

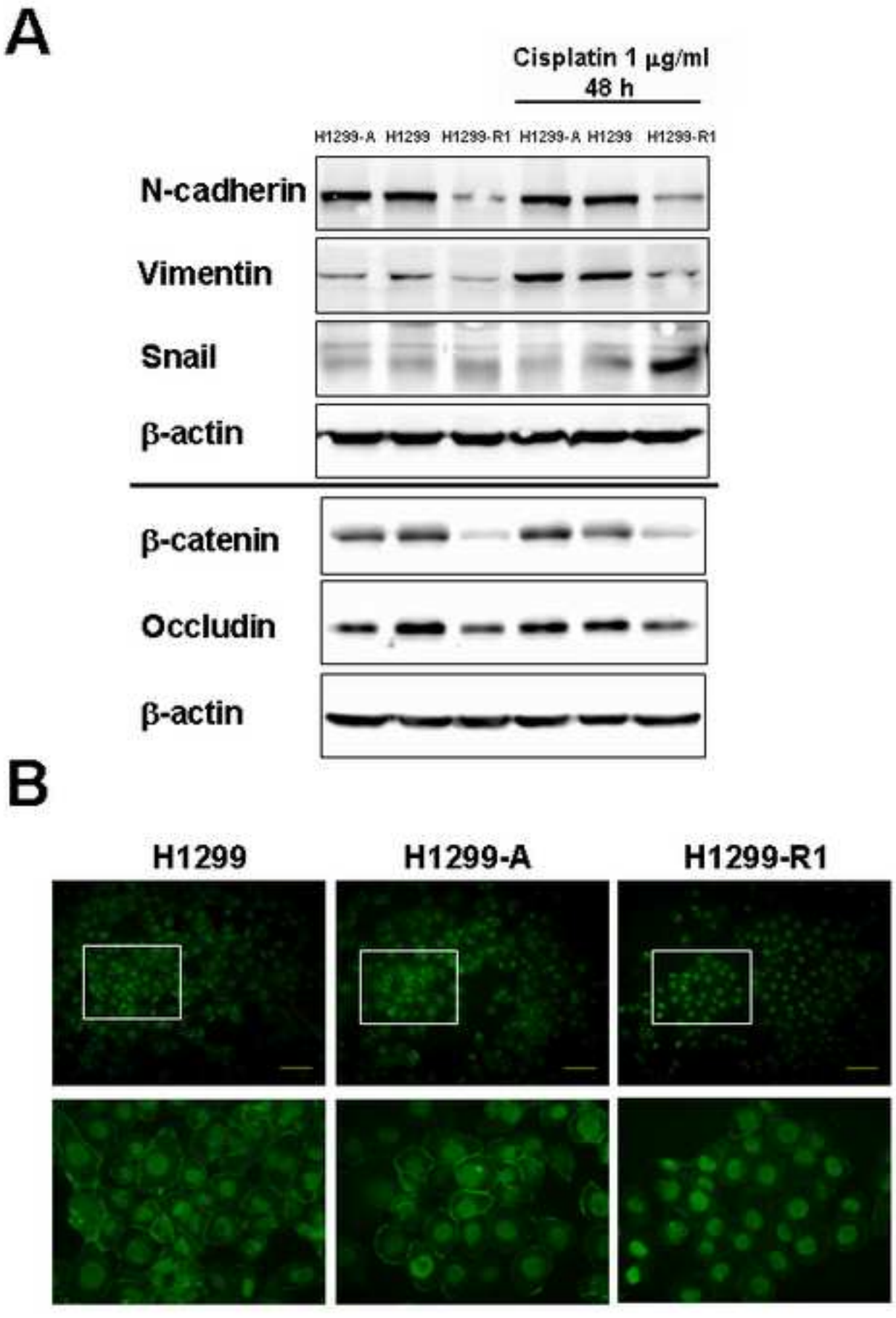

Figure 2

Click here to download high resolution image

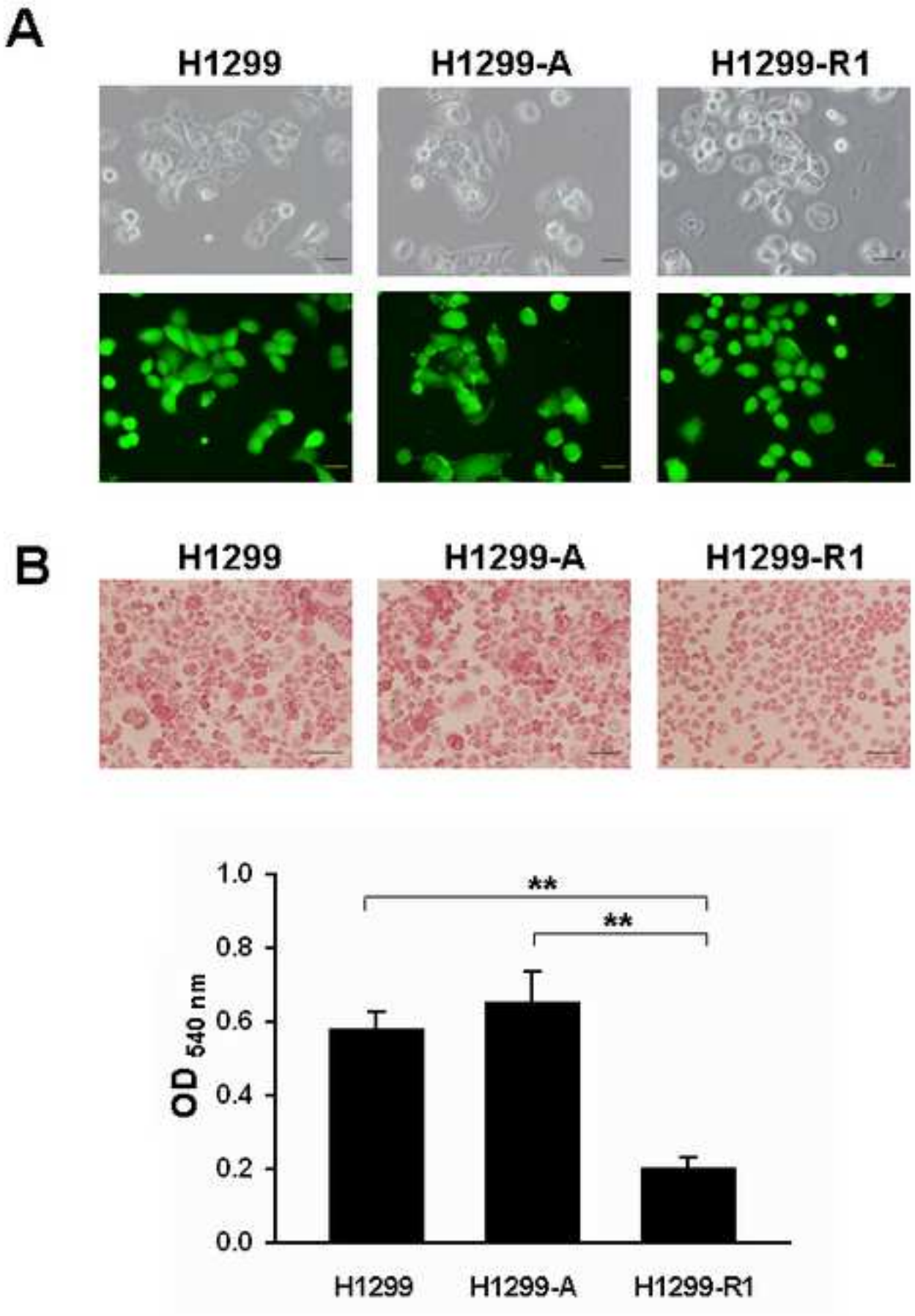

Figure 3

Click here to download high resolution image

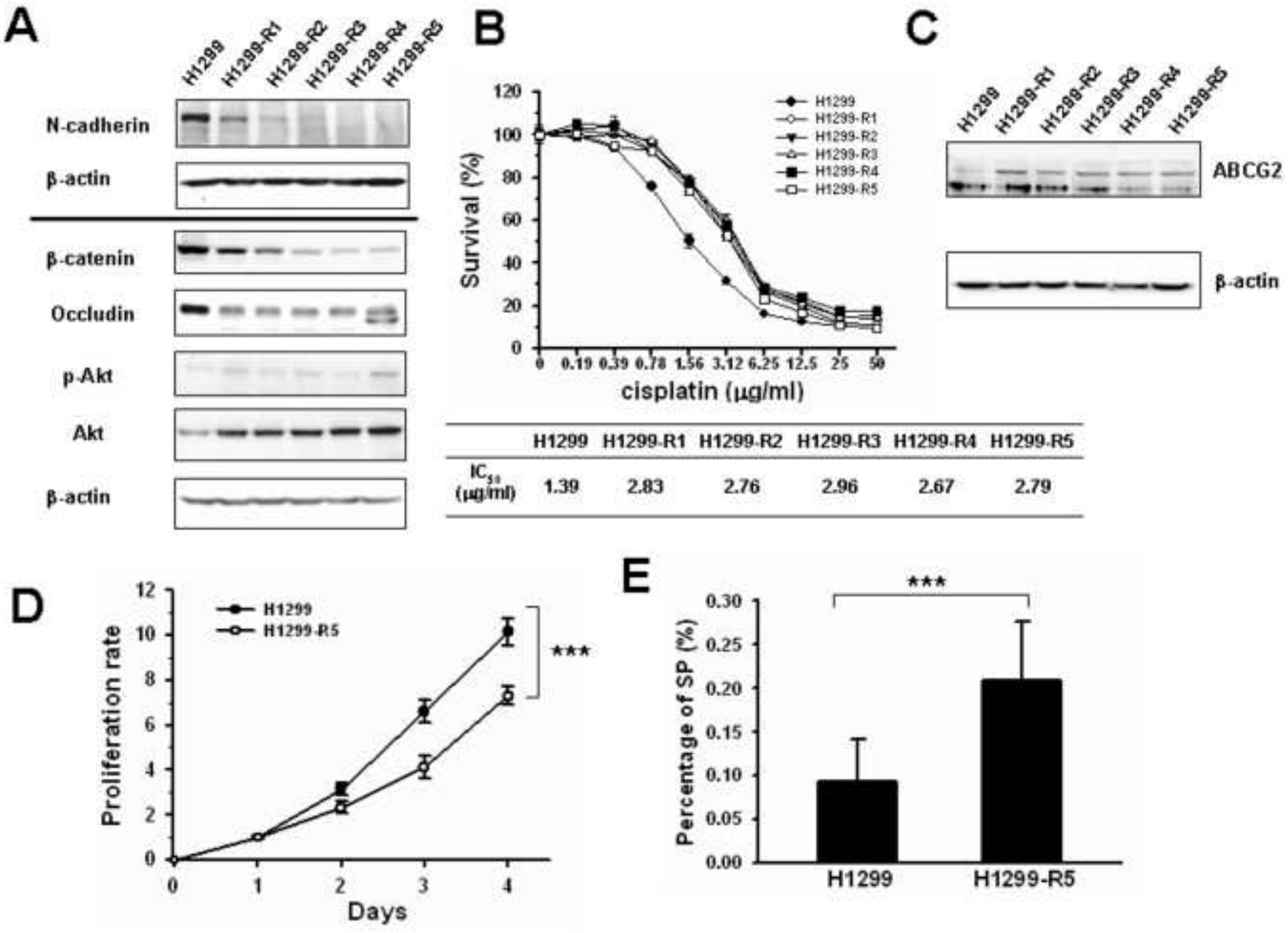

	H1299	H1299-R1	H1299-R2	H1299-R3	H1299-R4	H1299-R5
IC_{50} (μg/ml)	1.39	2.83	2.76	2.96	2.67	2.79

Figure 4

Click here to download high resolution image

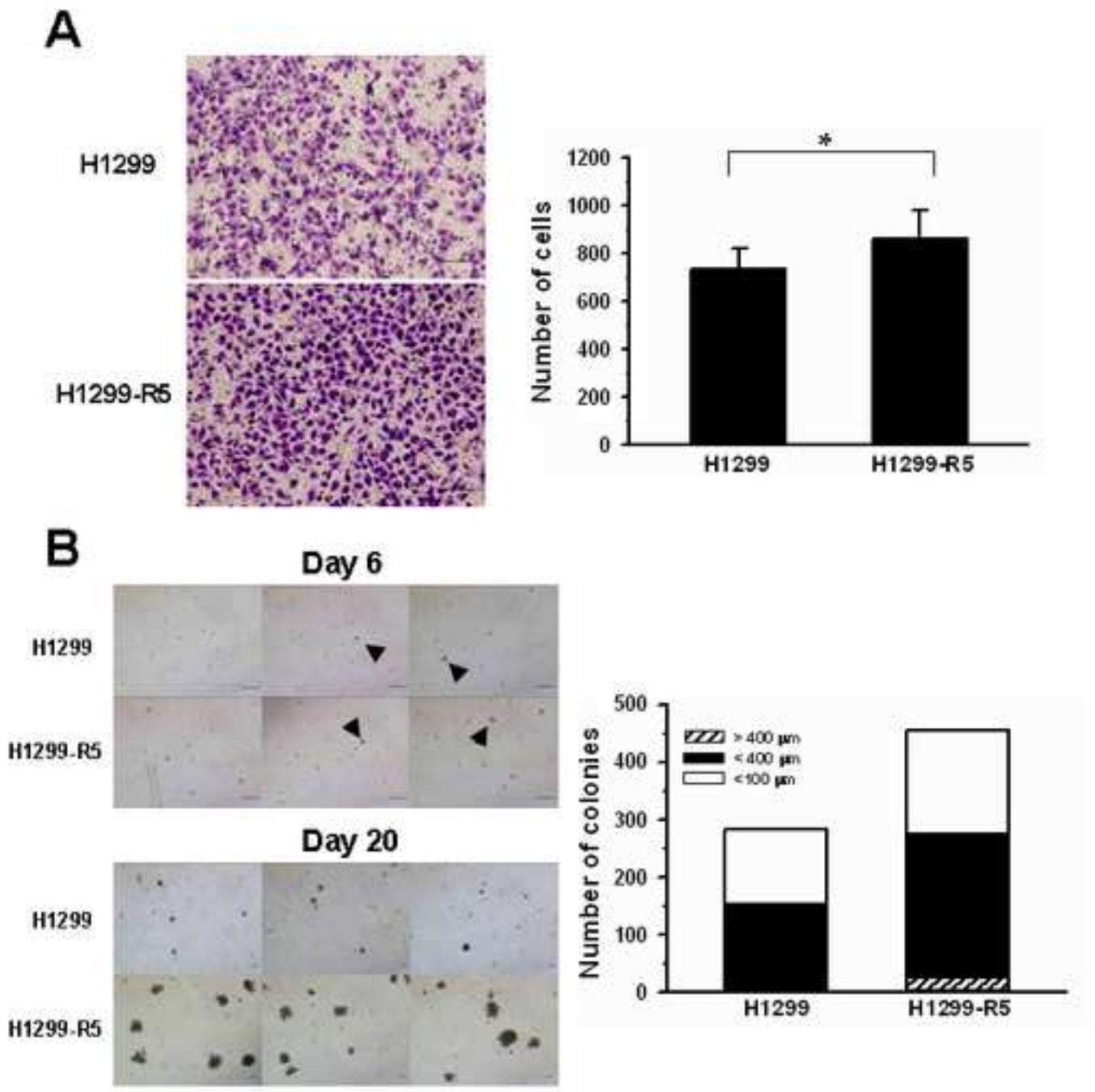

Figure 5

Click here to download high resolution image

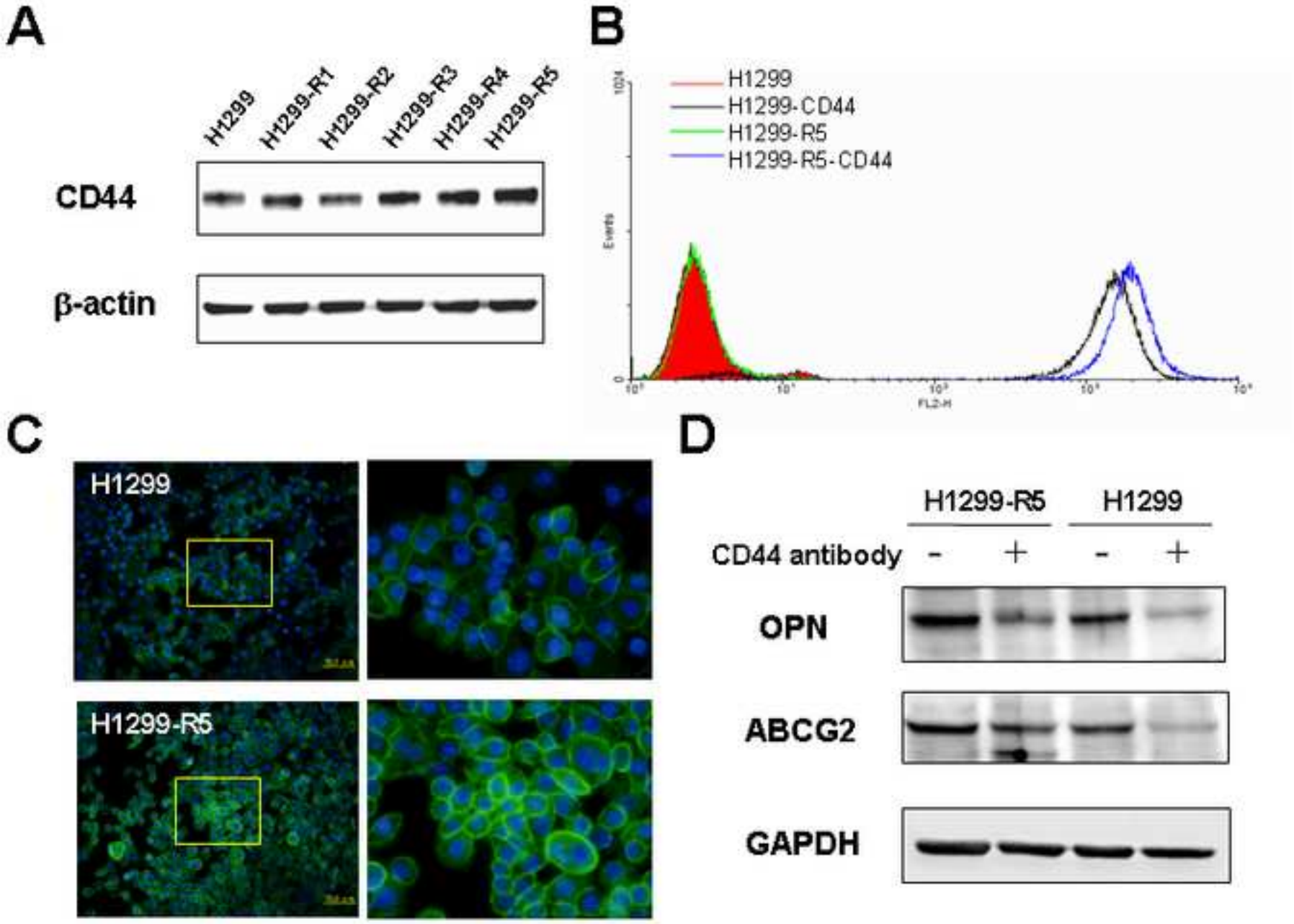

Figure 6

Click here to download high resolution image

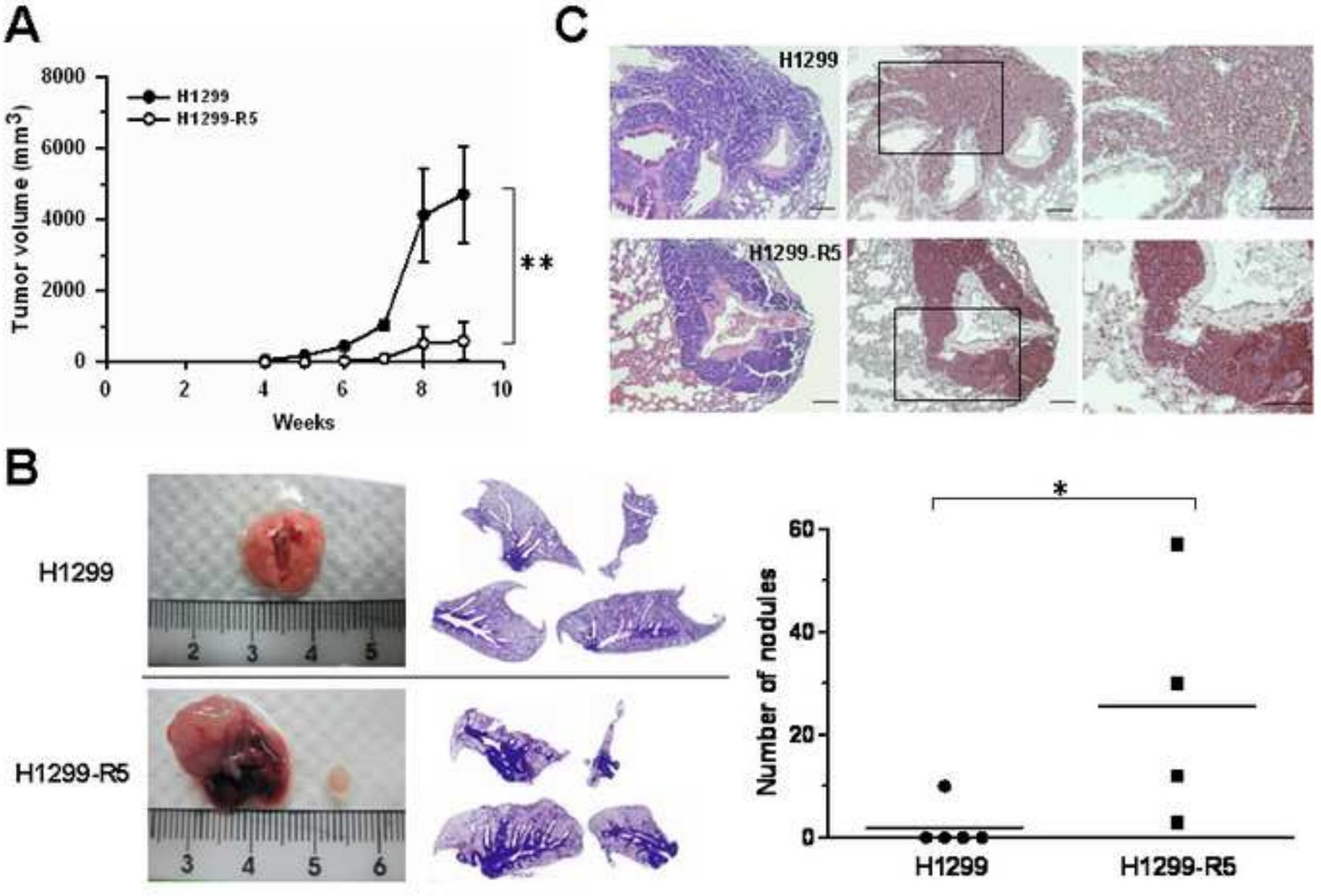

Supplementary Figure 1

Click here to download Supplementary File: sup.Fig. 1..tif

***Reviewer suggestions**

Reviewer suggestions for manuscript:

Rina Ohashi
rinaohas@med.juntendo.ac.jp

Parviz Behnam-Motlagh
parviz.behnam@medbio.umu.se

Esther P Black
Penni.Black@uky.edu

Heike Allgayer;
heike.allgayer@umm.de

Conflict of Interest

None of the authors have financial relationship with a commercial entity that has an interest in the content of this manuscript.